Organic Chemistry of Graphene: The Diels–Alder Reaction

ARTICLE *in* CHEMISTRY - A EUROPEAN JOURNAL · NOVEMBER 2013

Impact Factor: 5.73 · DOI: 10.1002/chem.201302622 · Source: PubMed

1 AUTHOR:

Pablo A. Denis
University of the Republic, Uruguay
104 PUBLICATIONS **1,529** CITATIONS

SEE PROFILE

CHEMISTRY
A EUROPEAN JOURNAL

FULL PAPER

DOI: 10.1002/chem.201302622

Organic Chemistry of Graphene: The Diels–Alder Reaction

Pablo A. Denis*[a]

Abstract: Herein, by using dispersion-corrected density functional theory, we investigated the Diels–Alder chemistry of pristine and defective graphene. Three dienes were considered, namely 2,3-dimethoxy-1,3-butadiene (DMBD), 9-methylanthracene (9MA), and 9,10-dimethylanthracene (910DMA). The dienophiles that were assayed were tetracyanoethylene (TCNE) and maleic anhydride (MA). When pristine graphene acted as the dienophile, we found that the cycloaddition products were 47–63 kcal mol^{-1} less stable than the reactants, thus making the reaction very difficult. The presence of Stone–Wales translocations, 585 double vacancies, or 555-777 reconstructed double vacancies did not significantly improve the reactivity because the cycloaddition products were still located at higher energy than the reactants. However, for the addition of 910DMA to single vacancies, the product showed comparable stability to the separated reactants, whereas for unsaturated armchair edges the reaction was extremely favorable. With regards the reactions with dienophiles, for TCNE, the cycloaddition product was metastable. In the case of MA, we observed a reaction product that was less stable than the reactants by 50 kcal mol^{-1}. For the reactions between graphene as a diene and the dienophiles, we found that the most-promising defects were single vacancies and unsaturated armchair edges, because the other three defects were much-less reactive. Thus, we conclude that the reactions with these above-mentioned dienes may proceed on pristine or defective sheets with heating, despite being endergonic. The same statement also applies to the dienophile maleic anhydride. However, for TCNE, the reaction is only likely to occur onto single vacancies or unsaturated armchair edges. We conclude that the dienophile character of graphene is slightly stronger than its behavior as a diene.

Keywords: cycloaddition · density functional calculations · Diels–Alder reactions · dienes · graphene

Introduction

Graphene, the "rising star" of the nanotechnological revolution,[1] is currently being considered as a key material for improving silicon-based electronic compounds.[2] However, it is well-known that the lack of a band gap renders such a goal difficult to achieve. A plethora of methods have been proposed to open up a band gap in graphene and to improve the "ON/OFF" ratio in graphene-based field-effect transistors. Among them, chemists have proposed the covalent functionalization of the sp^2 framework of graphene as a viable approach to fine-tune its electronic properties. Some of the chemical processes that have been proposed include: 1) radical-addition reactions, such as hydrogenation[3–5] and fluorination;[6–7] 2) organometallic chemistry,[8] by forming complexes with 3d transition metals and benzene; 3) organic chemistry of graphene. Thanks to the vast number of well-developed organic reactions, several procedures have been employed to functionalize graphene by using organic reagents. Without attempting to review all of them, we highlight the addition of aryl-diazonium salts,[9–12] alkylation,[13–14] 1,3-dipolar cycloaddition,[15–20] [2+2] cycloaddition,[21–23] [2+1] cycloaddition,[24–25] and the recently proposed reactions in which graphene can play the role of a diene or dienophile.[26–27] The first report on the diene and dienophile character of graphene was published by Sarkar et al.[26] In this work, these authors were able to reversible modify the electronic properties of graphene by the addition of dienes and dienophiles. The dienophiles that were investigated included tetracyanoethylene (TCNE) and maleic anhydride (MA), whilst the selected dienes were 9-methylanthracene (9MA) and 2,3-dimethoxy-1,3 butadiene (DMBD); highly oriented pyrolytic graphite (HOPG), exfoliated graphene, and epitaxial graphene were used. The powerful dienophile TCNE was attached to graphene at room temperature but, when heated at 100 °C, the reverse reaction occurred and the composite decomposed. On the addition of MA, the reactions required heat to proceed. Exfoliated graphene reacted at 130 °C, whilst epitaxial graphene needed less heat and the reaction took place at 70 °C. The cycloaddition products were stable up to 150 °C because the retro Diels–Alder reaction became dominant at this temperature. In terms of the performance of graphene as a dienophile, DMBD was attached to epitaxial graphene by heating at 50 °C. Such modification increased the electrical resistance by 60 %. The second diene that was employed was 9MA, which was successfully attached by heating in *p*-xylene at

[a] Dr. P. A. Denis
Computational Nanotechnology DETEMA
Facultad de Química, UDELAR, CC 1157
11800 Montevideo (Uruguay)
Fax: (+589) 229241906
E-mail: pablod@fq.edu.uy

130 °C for 12 h. The temperatures that were required to reverse the reactions with DMBD and 9MA were 170 and 160°, respectively, which were slightly higher than the corresponding reactions with dienophiles TCNE and MA. During the preparation of this manuscript, Bian et al.[27] reported the covalent patterning of cyclopentadienes (CPs) onto graphene surfaces by means of force-accelerated Diels–Alder reactions. The reactions took place exclusively on defects and edges. Chemical calculations showed that the edges of graphene acted as dienes, where the CP molecules attached, but the reaction did not take place on pristine graphene, because the reaction energies were unfavorable ($\Delta G°_{298} \approx +50$ kcal mol^{-1}). Interestingly, the results that were obtained by Sarkar et al.[26] and Bian et al.[27] present a very different scenario for the diene/dienophile character of graphene. On the one hand, Sarkar et al.[26] proposed that graphene could act as diene or dienophile under mild conditions. On the other hand, Bian et al.[27] used force-accelerated cycloaddition reactions and claimed that pristine graphene does not react at all with cyclopentadiene.

Previously, we have studied the chemical processes that graphene can undergo. We have shown that, for the addition of radicals, such as alkyl,[13] aryl,[12] and nitrene radicals,[24] the agglomeration of these groups increases the reaction energies, thereby facilitating the reactions. To our surprise, we observed similar behavior for [2+2] cycloaddition[22] and 1,3-dipolar cycloaddition reactions,[17,19] that is, the addition of one functional group activated the nearby C=C bonds and, thus, increased the reaction energies. In the particular case of the azomethine ylide, the reaction energy per functional group increased by almost 30 kcal mol^{-1}, if "armchair" lines were formed. This effect was used to explain the conflicting experimental and theoretical results. Motivated by the differences that were observed in the Diels–Alder chemistry of graphene by Sarkar et al.[26] and Bian et al.[27] and by the tremendous contribution that theoretical calculations have made to the field of nanotechnology,[28–43] we decided to continue our investigation into the reactivity of graphene by using dispersion-corrected density functional theory to investigate the diene and dienophile character of graphene. We expect that our work will shed light on this fascinating topic.

Methods

The sp^2 framework of graphene can interact through π-stacking and CH-π interactions with dienes and dienophiles. For this reason, it is essential to choose a method that can account for such dispersion interactions. We selected Zhao and Truhlar's M06L functional[44–45] for the periodic calculations because of its local character, which facilitates the inclusion of periodic conditions. The basis set that we selected was 6-31G*, as reported by Pople and co-workers.[46] To simulate infinite graphene sheets, we used 4×4, 5×5, and 6×6 supercells that contained 32, 50, and 72 atoms, respectively. 500 k-points were used to sample the unit cell and an ultrafine grid was employed. For comparative purposes, we performed cluster-model calculations by making use of a hydrogen-terminated $C_{48}H_{18}$ graphene flake. In this case, the more-accurate meta GGA M06-2X[44–45] method was selected. The M06L and M06-2X calculations were performed by using the Gaussian 09 program package.[47] In addition to the latter calculations, we also performed VDW-DF calculations as implemented in SIESTA.[48–49] We used the double-zeta basis set with polarization functions and fixed the orbital-confining cut-off to 0.01 Ry. The split norm that was utilized was 0.15. The DFT implementation in SIESTA can be prone to significant basis-set-superposition error (BSSE), even with relatively low degrees of radial confinement.[14] To avoid this problem, we used the counterpoise correction as suggested by Boys and Bernardi.[50] In all cases, we employed relaxed structures to estimate the BSSE-corrected binding energies and we took monomer-deformation energies into account. The interaction between ionic cores and valence electrons was described by Troullier–Martins norm-conserving pseudopotentials.[51] Geometry optimizations were performed by using the conjugate gradient algorithm until all of the residual forces were smaller than 0.01 eV Å^{-1}. We optimized the unit cells along the *a* and *b* axes, whilst the *c* axis was large enough to prevent interactions between adjacent sheets (25 Å). The unit cells were sampled by using a 30×30×1 Monkhorst–Pack sampling.

Results and Discussion

Graphene as a dienophile: We selected three dienes to study in the reaction with graphene, that is, 2,3-dimethoxy-1,3 butadiene (DMBD), 9-methylanthracene (9MA), and 9,10-dimethylanthracene (910DMA). The former two dienes were employed by Sarkar et al.[26] in their report about the Diels–Alder chemistry of graphene; 910DMA was also studied because its reaction with TCNE has been extensively studied and, thus, it serves the purpose of gauging the performance of a powerful dienophile. The reaction energies are listed in Table 1 and the optimized structures are shown in Figure 1. The cycloaddition reaction of DMBD with 4×4, 5×5, and 6×6 graphene models is extremely unfavorable. The reactants are located 37.5, 47.3, and 46.3 kcal mol^{-1} lower in energy than the reaction product for the 4×4, 5×5, and 6×6 unit cells, respectively. These values were somewhat expected, because an inspection of the bond lengths revealed that the carbon–carbon bond lengths between the carbon atoms of graphene and those of DMBD were 1.62 Å, which was extremely long for a carbon–carbon single bond. The low affinity between graphene and DMBD was confirmed by employing the VDW-DF/DZP and M06-2X functionals. This latter functional was more accurate than M06L. At the M06-2X level of theory, the addition of DMBD to a $C_{48}H_{18}$ graphene nanoflake is also not likely to occur in the central part of the cluster, because products are 23.7 kcal mol^{-1} higher in energy than reactants. If free-energy corrections are applied, the reaction is extremely endergonic, with

Table 1. Electronic binding energies [kcal mol^{-1}] for the addition of diene and dienophile groups to monolayer graphene.[a]

	2,3-Dimethoxy1,3-butadiene	9-Methyl-anthracene	9,10-Dimethyl-anthracene	TCNE	Maleic anhydride
benzene	+0.1 (COV)	+4.8 (COV)	+2.8	+2.2 (COV)	−4.4 (COV)
$C_{48}H_{18}$ nano-graphene	+23.7 (COV)	+41.7 (COV)	+46.3 (COV)	+52.5 (COV)	+46.2 (COV)
		−20.4 (ADS)	−21.5 (ADS)	−15.6 (ADS)	−10.2 (ADS)
G4×4	+37.5 (COV)				+49.6 (COV)
				−15.4 (ADS)	−10.4 (ADS)
G5×5	+47.3 (COV)	+59.1 (COV)	+65.6 (COV)	+63.2 (COV)	+49.7 (COV)
		−20.7 (ADS)	−22.1 (ADS)	−16.4 (ADS)	−10.3 (ADS)
G6×6	+46.3 (COV)				

[a] COV = covalent-addition complex, ADS = noncovalent complex. G$n\times n$ = graphene $n\times n$ unit cell. Positive reaction energy indicates that reactants are lower in energy than products.

were predicted for the infinite model and by using the M06L/6-31G* method. To assess the kinetic feasibility of the reactions with these two dienes, we determined the transition states for the Diels–Alder reactions of 9MA and 910DMA with graphene nanoflakes. Figure 2 shows the optimized structure for the cycloaddition product and the transition state in the reaction with 910DMA. At the

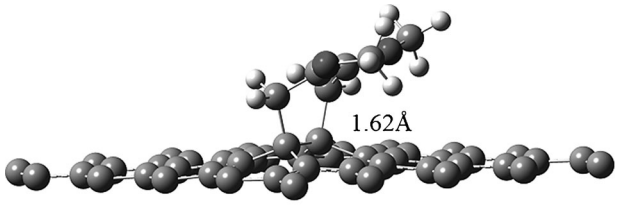

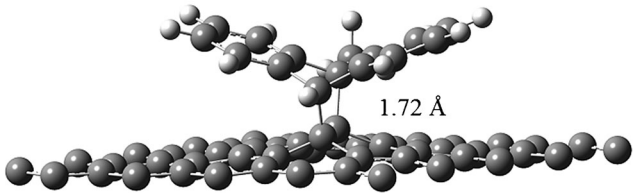

Figure 1. Optimized cycloaddition products for the reactions between graphene and 1,3-dimethyl butadiene (top) and 9-methylanthracene (bottom) at the M06L/6-31G* level of theory.

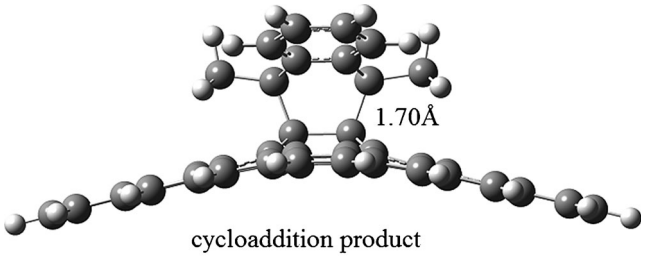

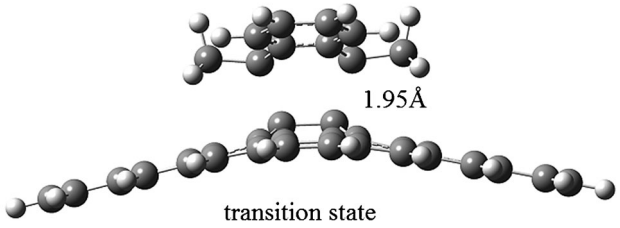

Figure 2. Optimized structures for the cycloaddition product and the transition state in the reaction between 9,10-dimethylanthracene and a $C_{48}H_{18}$ graphene nanoflake at the M06-2X/6-31G* level of theory.

a ΔG value of +48.3 kcal mol^{-1}. For the sake of completeness, we also studied the addition of DMBD to benzene. Even in this case, in which C_6H_6 is more reactive than graphene and the graphene flake, the reaction energy is −0.1 kcal mol^{-1} and, when entropy terms are included, it is endergonic, as described for the previous reaction.

For the other two dienes, that is, 9MA and 910DMA, we found that the reaction was more energetically hindered: The reaction energies for a 5×5 graphene unit cell with 9MA and 910DMA were 59.1 and 65.6 kcal mol^{-1}, respectively, both computed at the M06L/6-31G* level of theory. This result is in line with the predicted reaction energy for the $C_{48}H_{18}$ 4×4 graphene nanoflake, that is, 46.3 kcal mol^{-1}. 9MA and 910DMA formed strong dispersion-bound complexes with graphene. At the M06L/6-31G* level of theory, the adsorption energies onto graphene were −20.7 and −22.1 kcal mol^{-1} for 9MA and 910DMA, respectively. Rewardingly, the adsorption energies as determined at the M06-2X/6-31G* level of theory for these two molecules onto graphene nanoflakes were very similar to those that M06-2X/6-31G* level of theory, the transition states for the reactions with 9MA and 910DMA were located 45.3 and 49.2 kcal mol^{-1} higher in energy than the reactants, respectively, which corresponded to 65.7 and 70.7 kcal mol^{-1} higher in energy than the complexes that were bonded through π-stacking. The low reactivity of graphene as a dienophile could be compared with that of TCNE; thus, we investigated the reaction between TCNE and 910DMA. In contrast with the results that were obtained for graphene, this latter reaction was feasible from a thermodynamic standpoint, because the products were 36.5 kcal mol^{-1} more stable than the reactants at the M06-2X/6-31G* level of theory. Notwithstanding the energetic feasibility of this reaction, the carbon–carbon bond lengths between TCNE and 910DMA were 1.61 Å, which is very long for a carbon–carbon single bond. Again, we should not be surprised because the strength of formation of the two new carbon–carbon bonds is weak, because the TCNE and 910DMA are bonded by 36.5 kcal mol^{-1},

which corresponds to just 18.25 kcal mol^{-1} per carbon–carbon bond! As observed for graphene, there was a weakly bound complex with an interaction energy of −21.0 kcal mol^{-1}. Finally, we located the transition state of the reaction between TCNE and 910DMA. At the M06-2X/6-31G* level of theory, the transition state was located 9.9 kcal mol^{-1} lower in energy than the reactants and 11.1 kcal mol^{-1} higher in energy than the precursor complex. These results suggest that the reaction between graphene and the dienes requires some heating to proceed, because energy is required to form the new carbon–carbon bonds. This result is consistent with the work by Sarkar et al.,[26] who reported that the reactions with DMDB and 9MA required heating. Moreover, the weak interactions in the cycloaddition products are reflected by the low stability of the product under heating: The retro Diels–Alder reaction dominated at 150 °C.

Graphene as a diene: We considered the possibility of graphene acting as diene by using the same dienophiles as in the work of Sarkar et al.,[26] namely tetracyanoethylene (TCNE) and maleic anhydride (MA). The reaction energies are presented in Table 1. The cycloaddition product for the reaction between graphene and MA is shown in Figure 3. In this case, the carbon–carbon bonds are longer than those that were determined when graphene was the dienophile. At the M06L/6-31G* level of theory, the carbon–carbon bonds between graphene and MA were 1.67 Å. The reaction energy indicated that it was not likely to occur without heating, because the products were 49.7 kcal mol^{-1} higher in energy than the reactants. This result was also supported by the reaction energy as determined at the M06-2X/6-31G* level of theory for the reaction between MA and the graphene flake, that is, 46.2 kcal mol^{-1}. In contrast, the formation of a dispersion-bonded complex was more tempting because MA was adsorbed onto graphene with an interaction energy of −10.3 kcal mol^{-1} at the M06L/6-31G* level of theory or −10.2 kcal mol^{-1} at the M06-2X/6-31G* level of theory with the graphene nanoflake. In Figure 3, we also show the reaction pathway for the addition of MA to a 5×5 graphene unit cell. It can be clearly seen that the retro-Diels–Alder reaction has a low barrier, about 1.3 kcal mol^{-1}, at the M06L/6-31G* level of theory.

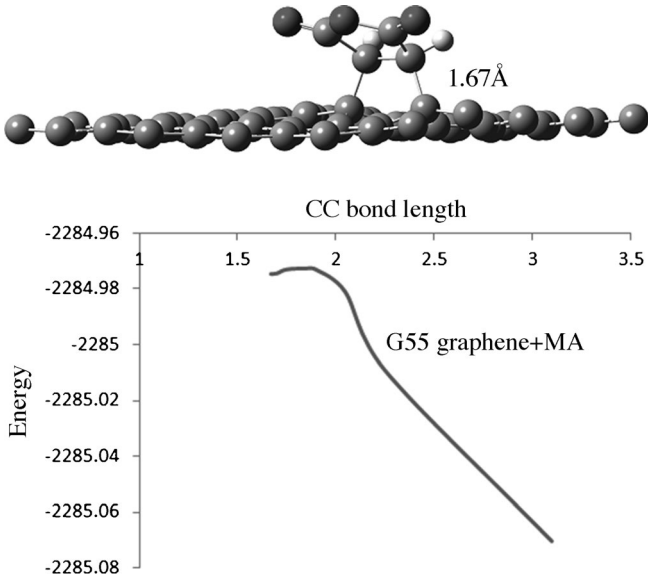

Figure 3. Optimized structure (top) and reaction pathway (bottom) for the addition of maleic anhydride to 5×5 graphene sheet, at the M06L/6-31G* level of theory.

The study of the reaction between graphene and TCNE was considerably more difficult. The first problem that we faced was that a minimum could not be found by performing traditional geometry optimizations at the M06L/6-31G*, M06-2X/6-31G*, or VDW-DF/DZP levels of theory. In all of our attempts, the calculation converged to a dispersion-bound complex. In the case of the 5×5 unit cell, the computed adsorption energy of TCNE onto graphene was −16.3 kcal mol^{-1} at the M06L/6-31G* level of theory. A similar value was determined by using the graphene nanoflake and the M06-2X/6-31G* method. To gain insight into the problem of whether the reaction product existed, we scanned the potential-energy surface at the M06L/6-31G* level of theory by fixing the carbon–carbon bond length between the infinite graphene sheet and TCNE. We also followed the same procedure at the M06-2X/6-31G* level of theory for the $C_{48}H_{18}$ graphene nanoflake. The reactions pathway are shown in Figure 4 and Figure 5. In both cases, we obtained similar results: The curve resembled an inflection point (as in, for example, the curve $y=x^3$). In the case of the graphene nanoflake, we calculated the vibrational frequencies for the point that was closer to the inflection point, which corresponded to a carbon–carbon bond length of 1.735 Å. This metastable structure is shown in Figure 6. We

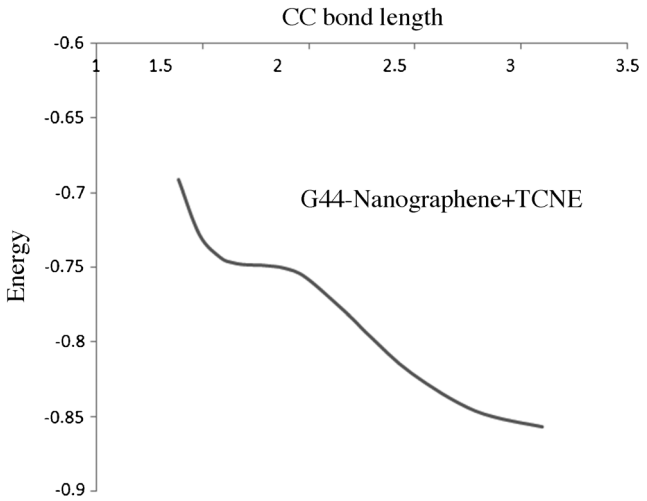

Figure 4. Reaction pathway for the addition of tetracyanoethylene to a 5×5 graphene sheet at the M06 L/6-31G* level of theory.

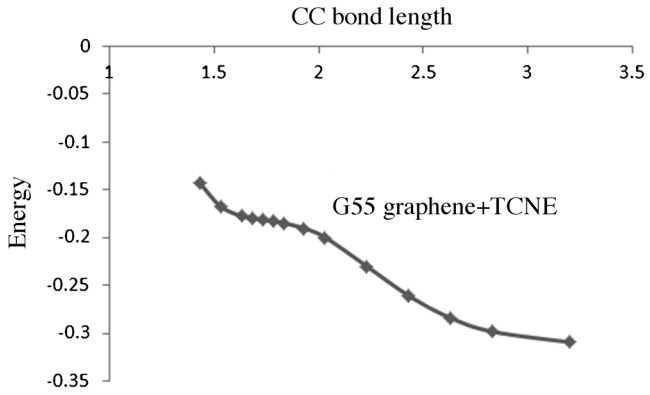

Figure 5. Reaction pathway for the addition of tetracyanoethylene to a $C_{48}H_{18}$ graphene nanoflake at the M06-2X/6-31G* level.

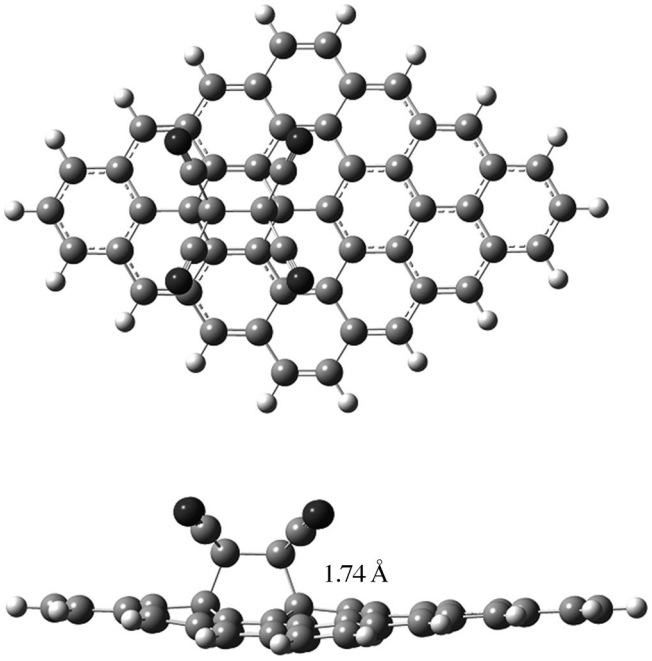

Figure 6. Optimized metastable cycloaddition product for the reaction between graphene and tetracyanoethylene at the M06-2X/6-31G* level of theory; the product was obtained with a relaxed reaction path scan.

found that this structure was a true minimum on the potential-energy surface, because all of the frequencies were real, the low frequencies were small, and the convergence criteria were accomplished. Yet, this structure was still metastable because it rapidly converged into the dispersion-bound complex. This finding was in disagreement with the results obtained by Sarkar et al.,[26] which indicated that the reaction proceeded at room temperature and without heating. We note that, in this case, the cycloaddition product was more unstable than those that were obtained when graphene worked as a dienophile, given that it decomposed at a lower temperature of 100 °C. As for MA, we agreed with the result by Sarkar et al.[26] which indicated that reaction needed heating to proceed.

Addition of dienes to defects: Because the reaction energies for the additions of DMDB, 9MA, and 91DMA were a little unfavorable and considering that experiments had confirmed that the reaction proceeded easily, we took into account the addition of 910DMA to defect sites and edges. The defects that were studied where those that were more popular and have been imaged by using aberration-corrected HRTEM, that is, single vacancies, 585 double vacancies, 555-777 reconstructed double vacancies, and Stone–Wales defects. The reaction energies are listed in Table 2.

Table 2. Electronic binding energies for the additions of tetracyanoethylene and 9,10-dimethylanthracene onto defective monolayer graphene.

G55 graphene 9,10-Dimethylanthracene	Site	Binding energy [kcal mol^{-1}]
pristine	1	+65.6 (COV)
		−22.1 (ADS)
Stone–Wales defect	1	+22.2 (COV)
	2	+30.1
585 double vacancy	1	+30.7
555-777 double vacancy	1	+48.6
single vacancy	1	−1.0
TCNE		
pristine	1	+63.2 (COV)
		−16.4 (ADS)
Stone–Wales defect	1	−18.2 (ADS)
	2	−17.6 (ADS)
585 double vacancy	1	+23.0 (COV)
	2	−15.2 (ADS)
	3	+36.8 (COV)
555-777 double vacancy	1	+42.6 (COV)
	2	−17.3 (ADS)
single vacancy	1	−37.9 (COV)
	2	+0.5 (COV)
	3	−13.8

910DMA attached onto the part of the defect that had the shortest C=C bond. The attachment sites are shown in Figure 7. In the case of the Stone–Wales defect, 910DMA attached onto the carbon−carbon bond that connected two pentagons. As observed for pristine graphene, the cycloaddition products were higher in energy than the reactants, but, in this case, the relative energy was smaller, 22.2 kcal mol^{-1}, which was about half that of the value for the pristine sheet. The 585 and 555-777 defects were also very unreactive, because the reactants were more stable than the products by 30.7 and 48.6 kcal mol^{-1}. The most-reactive defect was the single vacancy, for which the reactants and products had similar energies. Yet, when free-energy corrections were included, the reaction became endergonic, because the entropic term was unfavorable. Finally, we studied the addition of 9MA to bare and saturated armchair and zigzag edges. These processes were investigated by using infinite armchair carbon nanoribbons that were similar to those used in our recent work on arylated graphene.[13] We found that the reaction was favorable when it occurred on unsaturated edges. At the VDW-DF/DZP level the reaction energies were

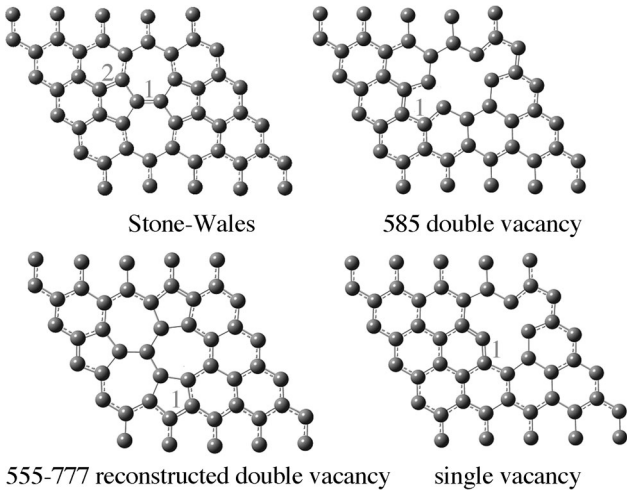

Figure 7. Selected C=C double bonds in defective graphene for addition of the 9,10-dimethylanthracene diene; the selected C=C bonds are the shortest ones.

−42.1 and +6.13 kcal mol^{-1}, for bare and saturated armchair edges, respectively.

Addition of dienophiles to defects: In contrast with the experimental results, we found that the addition of TCNE was quite troublesome. However, when defects were present, the situation changed to a certain extent. The reaction energies are listed in Table 2. For the Stone–Wales defect, two sites were studied, as shown in Figure 8. In both cases, we found

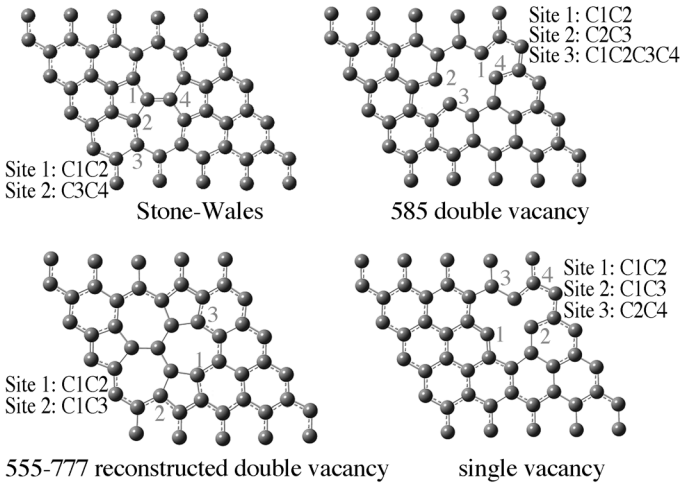

Figure 8. Selected C=C−C=C regions in defective graphene for addition to the tetracyanoethylene dienophile; the diene region is limited by the number of carbon atoms that are involved.

that TCNE was noncovalently adsorbed instead of covalently bonded. In the case of the 585 double vacancy, three sites were selected. In two of them, TCNE was covalently bonded, but again the products were less stable than the reactants by 23 and 36.8 kcal mol^{-1}, respectively. The 555-777 reconstructed double vacancy was less reactive. In one case, TCNE was adsorbed, whereas, in the other case, the cycloaddition product was 42.6 kcal mol^{-1} less stable than the reactants. As observed for 910DMA, the single vacancy was more reactive. Although at site 1, the carbon−carbon bonds were not conjugated, the addition of TCNE gave a cycloaddition product that was 37.9 kcal mol^{-1} more stable than the reactants. At site 2, which more-resembled a diene, the products had almost the same energy as the reactants. The large reaction energy at site 1 was attributed to the fact that TCNE was bonded to two carbon atoms that were linked to the missing carbon atom; thus, they were extremely reactive. In light of these results, the addition of TCNE likely occurred without heating at only single vacancies or edges with a similar structure as the single vacancy. For example, at the VDW-DF/DZP level of theory and by using the same ribbons as in previous calculations,[13] we found that TCNE added onto an unsaturated armchair edge of an armchair ribbon with a reaction energy of −40.1 kcal mol^{-1}, at the VDW-DF/DZP level of theory. However, if the edge of the ribbon was saturated with an H atom, the reaction was endergonic since the reaction energy was +21.0 kcal mol^{-1}; these evidence reveal that graphene is a weak diene.

Conclusion

The Diels–Alder chemistry of graphene was studied by employing dispersion-corrected density functional theory and by using infinite graphene models, as well as graphene nanoflakes. When graphene played the role of the dienophile, we found that DMBD, 9MA, and 910DMA formed cycloaddition products that were 47–63 kcal mol^{-1} less stable than the reactants, thus making the reactions unlikely. When defect sites were considered, the presence of Stone–Wales translocations, 585 double vacancies, or 555-777 reconstructed double vacancies did not change the overall picture because the cycloaddition products were located higher in energy than the reactants. However, for the addition of 910DMA to single vacancies, we found that the product was as stable as the separated reactants. The addition of 9MA was only exergonic when it was attached to bare edges. If graphene was reacted with dienophiles, the situation became more complicated, because, for the powerful dienophile TCNE, the cycloaddition product was metastable. Although we were able to find a reaction product for the reaction with maleic anhydride, it was less stable than the reactants by 50 kcal mol^{-1}. As observed for the reaction of graphene with dienes, we found that the most-promising defects for reaction with dienophiles were single vacancies and unsaturated armchair edges, because the other three defects were much less reactive. On the basis of these calculations, we conclude that the reactions with these dienes may proceed on pristine or defective sheets with heating, even though they are endergonic. The same statement applies to the dienophile maleic anhydride. However, for TCNE, the reaction on the pristine sheet is extremely unlikely, even under heating. TCNE is only attached onto single vacancies or edges with similar structures to the single vacancies, that is, not saturated with

H atoms. Thus, the dienophilic character of graphene is slightly stronger than its behavior as a diene.

Acknowledgements

The author thanks the PEDECIBA Quimica for financial support. The author thanks Walter Shands from Intel for his help with Intel Cluster Studio.

[1] R. F. Service, *Science* **2009**, *324*, 875–877.
[2] F. Schwierz, *Nat. Nanotechnol.* **2010**, *5*, 487–496.
[3] D. C. Elias, R. R. Nair, T. M. G. Mohiuddin, S. V. Morozov, P. Blake, M. P. Halshall, A. C. Ferrari, D. W. Boukhvalov, M. I. Katsnelson, A. K. Geim, K. S. Novoselov, *Science* **2009**, *323*, 610.
[4] J. O. Sofo, A. S. Chaudhari, G. D. Barber, *Phys. Rev. B* **2007**, *75*, 153401.
[5] P. A. Denis, F. Iribarne, *J. Mol. Struct.* **2009**, *907*, 93.
[6] H. Y. Liu, Z. F. Hou, C. H. Hu, Y. Yang, Z. Z. Zhu, *J. Phys. Chem. C* **2012**, *116*, 18193.
[7] D. K. Samarakoon, Z. Chen, C. Nicolas, X. Q. Wang, *Small* **2011**, *7*, 965–969.
[8] S. M. Avdoshenko, I. N. Ioffe, G. Cuniberti, L. Dunsch, A. A. Popov, *ACS Nano* **2012**, *9*, 9939.
[9] J. R. Lomeda, C. D. Doyle, D. V. Kosynkin, W. F. Hwang, J. M. Tour, *J. Am. Chem. Soc.* **2008**, *130*, 16201.
[10] E. Bekyarova, M. E. Itkis, P. Ramesh, C. Berger, M. Sprinkle, W. A.de Heer, R. C. Haddon, *J. Am. Chem. Soc.* **2009**, *131*, 1336.
[11] R. Sharma, J. H. Baik, C. J. Perera, M. S. Strano, *Nano Lett.* **2010**, *10*, 398.
[12] P. A. Denis, *ChemPhysChem* **2013**, *14*, 3271–3277.
[13] P. A. Denis, F. Iribarne, *Chem. Eur. J.* **2012**, *18*, 7568.
[14] L. Liao, Z. Song, Y. Zhou, H. Wang, Q. Xie, H. Peng, Z. Liu, *Small* **2013**, *9*, 1348–1352.
[15] V. Georgakilas, A. B. Bourlnos, R. Zboril, T. A. Steriotis, P. Dallas, A. K. Stubos, C. Trapalis, *Chem. Commun.* **2010**, *46*, 1766.
[16] M. Quintana, K. Spyrous, M. Grzelczak, W. R. Browne, P. Rudolf, M. Prato, *ACS Nano* **2010**, *4*, 3527.
[17] P. A. Denis, F. Iribarne, *Int. J. Quantum Chem.* **2010**, *110*, 1764.
[18] Y. Cao, K. N. Houk, *J. Mater. Chem.* **2011**, *21*, 1503.
[19] P. A. Denis, F. Iribarne, *Chem. Phys. Lett.* **2012**, *550*, 111–117.
[20] Y. Yuan, P. Chen, X. Ren, H. Wang, *ChemPhysChem* **2012**, *13*, 741–750.
[21] X. Zhong, J. Jin, S. Li, Z. Niu, W. Hu, R. Li, J. Ma, *Chem. Commun.* **2010**, *46*, 7340.
[22] P. A. Denis, F. Iribarne, *J. Mater. Chem.* **2012**, *22*, 5470–5477.
[23] I. V. Magedov, L. V. Frolova, M. Ovezmyradov, D. Bethke, E. A. Shaner, N. G. Kalugin, *Carbon* **2013**, *54*, 192–200.
[24] P. A. Denis, F. Iribarne, *J. Phys. Chem. A J. Phys. Chem. B J. Phys.-Chem. C* **2011**, *115*, 195.
[25] K. Suggs, D. X. Reuven, Q. Wang, *J. Phys. Chem. C* **2011**, *115*, 3313.
[26] S. Sarkar, E. Bekyarova, S. Niyogi, R. C. Haddon, *J. Am. Chem. Soc.* **2011**, *133*, 3324–3327.
[27] S. Bian, A. M. Scott, Y. Cao, Y. Liang, S. Osuna, K. N. Houk, A. B. Braunschweig, *J. Am. Chem. Soc.* **2013**, *135*, 9240–9243.
[28] N. Ghaderi, M. Peressi, *J. Phys. Chem. C* **2010**, *114*, 21625.
[29] P. A. Denis, *J. Phys. Chem. A J. Phys. Chem. B J. Phys.Chem. C* **2009**, *113*, 5612.
[30] P. A. Denis, R. Faccio, A. W. Mombru, *ChemPhysChem* **2009**, *10*, 715.
[31] P. A. Denis, *Chem. Phys. Lett.* **2010**, *492*, 251.
[32] P. A. Denis, *Chem. Phys. Lett.* **2011**, *508*, 95.
[33] P. A. Denis, F. Iribarne, *J. Mol. Struct.* **2009**, *907*, 93.
[34] P. A. Denis, F. Iribarne, *J. Mol. Struct.* **2010**, *957*, 114.
[35] P. Chandrachud, B. S. Pujari, S. Haldar, B. Sanyal, D. K. Kanhere, *J. Phys. Condens. Matter* **2010**, *22*, 465502.
[36] N. Al-Aqtash, I. Vasiliev, *J. Phys.Chem. C* **2009**, *113*, 12970.
[37] J. Dai, J. Yuan, P. Giannozzi, *Appl. Phys. Lett.* **2009**, *95*, 232105.
[38] J. Dai, J. Yuan, *J. Phys. Condens. Matter* **2010**, *22*, 225501.
[39] Z. M. Ao, J. Yang, S. Li, Q. Jiang, *Chem. Phys. Lett.* **2008**, *461*, 276.
[40] Z. M. Ao, J. Yang, S. Li, Q. Jiang, *Phys. Chem. Chem. Phys.* **2009**, *11*, 1683.
[41] S. J. Gong, W. Sheng, J. H. Chu, *J. Phys. Condens. Matter* **2010**, *22*, 245502.
[42] F. T. Wang, L. Chen, C. J. Tian, Y. Meng, Z. G. Wang, R. Q. Zhang, M. X. Jin, P. Zhang, D. J. Ding, *J. Comput. Chem.* **2011**, *32*, 3264.
[43] V. V. Ivanovskaya, A. Zobelli, D. Teillet-Billy, N. Rougeau, V. Sidis, P. R. Briddon, *Eur. Phys. J. B* **2010**, *76*, 481.
[44] Y. Zhao, D. G. Truhlar, *J. Chem. Phys.* **2006**, *125*, 194101.
[45] Y. Zhao, D. G. Truhlar, *Acc. Chem. Res.* **2008**, *41*, 157–167.
[46] R. Ditchfield, W. J. Hehre, J. A. Pople, *J. Chem. Phys.* **1971**, *54*, 724.
[47] Gaussian 09, Revision A.1, M. J. Frisch, G. W. Trucks, H. B. Schlegel, G. E. Scuseria, M. A. Robb, J. R. Cheeseman, G. Scalmani, V. Barone, B. Mennucci, G. A. Petersson, H. Nakatsuji, M. Caricato, X. Li, H. P. Hratchian, A. F. Izmaylov, J. Bloino, G. Zheng, J. L. Sonnenberg, M. Hada, M. Ehara, K. Toyota, R. Fukuda, J. Hasegawa, M. Ishida, T. Nakajima, Y. Honda, O. Kitao, H. Nakai, T. Vreven, J. A. Montgomery, Jr., J. E. Peralta, F. Ogliaro, M. Bearpark, J. J. Heyd, E. Brothers, K. N. Kudin, V. N. Staroverov, R. Kobayashi, J. Normand, K. Raghavachari, A. Rendell, J. C. Burant, S. S. Iyengar, J. Tomasi, M. Cossi, N. Rega, J. M. Millam, M. Klene, J. E. Knox, J. B. Cross, V. Bakken, C. Adamo, J. Jaramillo, R. Gomperts, R. E. Stratmann, O. Yazyev, A. J. Austin, R. Cammi, C. Pomelli, J. W. Ochterski, R. L. Martin, K. Morokuma, V. G. Zakrzewski, G. A. Voth, P. Salvador, J. J. Dannenberg, S. Dapprich, A. D. Daniels, Ö. Farkas, J. B. Foresman, J. V. Ortiz, J. Cioslowski, D. J. Fox, Gaussian, Inc., Wallingford CT, **2009**.
[48] J. M. Soler, E. Artacho, J. D. Gale, A. Garcia, J. Junquera, P. Ordejon, D. Sanchez-Portal, *J. Phys. Condens. Matter* **2002**, *14*, 2745.
[49] P. Ordejón, E. Artacho, J. M. Soler, *Phys. Rev. B* **1996**, *53*, R10441.
[50] F. S. Boys, F. Bernardi, *Mol. Phys.* **1970**, *19*, 553.
[51] N. Troullier, J. L. Martins, *Phys. Rev. B* **1991**, *43*, 1993.

Received: July 5, 2013
Published online: October 2, 2013

